

Development and Comparative Studies of Three Non-free Parameter Lattice Boltzmann Models for Simulation of Compressible Flows

L. M. Yang¹, C. Shu^{2,*} and J. Wu¹

¹ Department of Aerodynamics, College of Aerospace Engineering, Nanjing University of Aeronautics and Astronautics, Yudao Street, Nanjing 210016, Jiangsu, China

² Department of Mechanical Engineering, National University of Singapore, 10 Kent Ridge Crescent, Singapore 119260, Singapore

Received 17 September 2011; Accepted (in revised version) 9 November 2011

Available online 10 July 2012

Abstract. This paper at first shows the details of finite volume-based lattice Boltzmann method (FV-LBM) for simulation of compressible flows with shock waves. In the FV-LBM, the normal convective flux at the interface of a cell is evaluated by using one-dimensional compressible lattice Boltzmann model, while the tangential flux is calculated using the same way as used in the conventional Euler solvers. The paper then presents a platform to construct one-dimensional compressible lattice Boltzmann model for its use in FV-LBM. The platform is formed from the conservation forms of moments. Under the platform, both the equilibrium distribution functions and lattice velocities can be determined, and therefore, non-free parameter model can be developed. The paper particularly presents three typical non-free parameter models, D1Q3, D1Q4 and D1Q5. The performances of these three models for simulation of compressible flows are investigated by a brief analysis and their application to solve some one-dimensional and two-dimensional test problems. Numerical results showed that D1Q3 model costs the least computation time and D1Q4 and D1Q5 models have the wider application range of Mach number. From the results, it seems that D1Q4 model could be the best choice for the FV-LBM simulation of hypersonic flows.

AMS subject classifications: 76T10

Key words: FV-LBM, non-free parameter models, compressible inviscid flows.

1 Introduction

In recent years, the lattice Boltzmann method (LBM) has attracted growing attentions

*Corresponding author.

URL: <http://serve.me.nus.edu.sg/shuchang/>

Email: mpeshuc@nus.edu.sg (C. Shu)

as an alternative approach to simulate fluid flows [1–4]. Unlike conventional numerical methods, which are based on discretization of macroscopic conservation equations, the LBM directly solves the kinetic equations at mesoscopic level. The appealing merits of LBM are the simple algebraic operation, linear convective terms and easy parallelism. Thanks to such advantages, LBM has got a lot of achievements in various fields, such as in isothermal incompressible flows [5, 6], turbulent flows [7, 8], multi-phase flows [9–11], etc.

However in the field of compressible flow simulation, the applications of LBM are still limited. Among limited works [12–16], the discrete velocity Boltzmann equation (DVBE) is usually solved. Kataoka and Tsutahara [12, 13] firstly proposed a method that utilizes the Crank-Nicolson scheme to solve DVBE to obtain the solution of flow field. Later, Qu et al. [14] presented a second-order TVD scheme to solve DVBE. They also proposed an alternative scheme [15] that discretizes DVBE by finite volume method (FVM). Besides, Li et al. [16] introduced the implicit-explicit (IMEX) Runge-Kutta scheme, a recently developed numerical technique for stiff problems, to solve DVBE. It must be pointed out that DVBE is a set of partial differential equations. The number of unknowns in DVBE (same as the number of lattice velocities) is much larger than that (number of conservative variables) in the macroscopic governing equations. In addition, the time step used for solving DVBE is usually very small due to severe stability condition. These lead to the solution of DVBE very inefficient. Another concern is that the multi-dimensional compressible lattice Boltzmann (LB) model is much more complicated than its one-dimensional counterpart. For example, the expressions of 2D equilibrium distribution functions shown in [14] are very complicated. This brings inconvenience for the application to solve multi-dimensional problems.

To avoid direct solution of DVBE, and in the meantime, to avoid application of multi-dimensional LB model, Ji et al. [17] proposed a finite volume-based lattice Boltzmann method (FV-LBM). In the FV-LBM, the LBM is used to construct flux solver at the interface, while the FVM is used to discretize the macroscopic governing equations. Hence, the advantages of two methods are well combined, i.e., efficient calculation of flux vectors and accurate simulation of all compressible features including shock, contact discontinuity and rarefaction wave by LBM and geometric flexibility by FVM. Apparently, the computational cost and virtual memory required by FV-LBM are far less than those of DVBE-based solvers [12–16] as the result of lesser variables involved. Moreover, the local time step and implicit residual smoothing scheme can also be applied to improve the computational efficiency. In the FV-LBM, only one-dimensional (1D) LB model is applied. Its one-dimensional application is quite straightforward. For the multi-dimensional case, the 1D LB model is applied along normal direction of the cell interface to evaluate the normal flux vectors. The flux vectors in the tangential direction are evaluated by using the same way as used in conventional Euler/Navier-Stokes (N-S) solvers. It should be indicated that although the idea of FV-LBM is given in [17], its details are not clearly shown. This paper will make up this scarcity and give details of FV-LBM.

So far, in the application of FV-LBM, the 1D LB models of Kataoka and Tsuta-

hara [12, 13] and Qu et al. [14, 15] have been successfully applied to simulate some 1D and 2D compressible flows with shock waves and contact discontinuities. However, when these models are applied to problems with high Mach number, the computation may either diverge or lead to unphysical solution. Through numerical experiments, it was found that the magnitude of lattice velocity used in the LB model has a great effect on the applicability of the model for high Mach number cases. As the lattice velocity is specified beforehand by the user, one has to fine tune its value in order to simulate compressible flows with higher Mach number. This brings us a question: how to properly choose the lattice velocity of 1D LB model in the application of FV-LBM? To answer this question, this paper proposes a platform to automatically determine the lattice velocity from the high order momentum conservation forms.

In the platform, we use the conservation forms of moments to form an equation system, where both the equilibrium distribution functions and lattice velocities are considered as unknowns, which are solved from the system. Under the platform, we can develop different 1D LB models. As no free parameter is appeared in these models, we call them non-free parameter models. In this work, three typical non-free parameter models, i.e., D1Q3, D1Q4 and D1Q5, are presented under the platform. Their performances in terms of accuracy, computational efficiency and application range of Mach number will be comparatively studied for the test 1D and 2D problems.

2 Methodology

2.1 A finite volume-based lattice Boltzmann method (FV-LBM)

In this paper, we focus on the simulation of compressible inviscid flows. Considering compressible Euler equation, its discrete expression in the form of FVM is given by

$$\frac{d\vec{W}_I}{dt} = -\frac{1}{\Omega_I} \sum_{i=1}^{N_f} \vec{F}_i S_i, \quad (2.1)$$

where I is the index for a control volume, \vec{W} and \vec{F} are the vector of conservative variables and convective flux vector, respectively. In general, these vectors can be written as the three-dimensional form of the following five components

$$\vec{W} = \begin{bmatrix} \rho \\ \rho u \\ \rho v \\ \rho w \\ \rho E \end{bmatrix}, \quad \vec{F} = \begin{bmatrix} \rho V \\ \rho u V + n_x p \\ \rho v V + n_y p \\ \rho w V + n_z p \\ (\rho E + p)V \end{bmatrix}, \quad (2.2)$$

where, (u, v, w) and (n_x, n_y, n_z) denote the velocity vector and unit normal vector of the surface of the control volume in Cartesian coordinate system, respectively. V represents the contravariant velocity, which is defined as the scalar product of the velocity

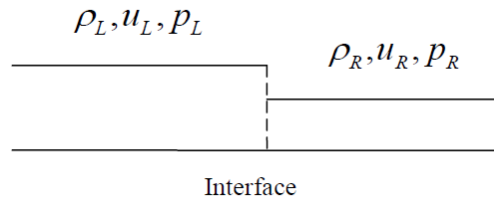


Figure 1: Configuration a Riemann problem.

vector and the unit normal vector, i.e.,

$$V = n_x u + n_y v + n_z w, \tag{2.3}$$

ρ , p and E are the density, pressure and total energy of the mean flow, respectively. The total energy E can be obtained from the formula

$$E = \frac{p}{(\gamma - 1)\rho} + \frac{1}{2}(u^2 + v^2 + w^2). \tag{2.4}$$

Furthermore, Ω_I and N_f represent the volume and the number of the faces of the control volume I , respectively. S_i denotes the area of the i th face of the control volume.

In Eq. (2.1), the key issue is how to design an appropriate flux solver to evaluate the convective fluxes \vec{F} . Among available flux solvers, Roe scheme [18], van Leer scheme [19] and advection upstream splitting method (AUSM) [20–22], are probably the most popular schemes in the evaluation of convective fluxes. However, the major deficiency of them is that the nonlinear convective terms have to be considered in the computation. On the contrary, it is known that the convective terms of LBM are linear. This feature may make flux calculation by LBM easier. The lattice Boltzmann equation (LBE) with Bhatnagar-Gross-Krook (BGK) collision model [23] gives

$$f_\alpha(r + e_\alpha \delta t, t + \delta t) - f_\alpha(r, t) = \frac{1}{\tau}(g_\alpha(r, t) - f_\alpha(r, t)), \tag{2.5}$$

where, f_α is the distribution function in the α th direction, g_α is its corresponding function at equilibrium state. e_α is the lattice velocity in the α th direction, and τ is relevant to the single relaxation time and streaming time step δt .

In the simulation of inviscid flows, the collision term of LBE which corresponds to the viscous term of N-S equations can be ignored. Consequently, the distribution function can be approximated by its corresponding form at equilibrium state ($f_\alpha = g_\alpha$). That is, Eq. (2.5) reduces to

$$g_\alpha(r, t) = g_\alpha(r - e_\alpha \delta t, t - \delta t), \tag{2.6}$$

where, r denotes the position of interface of control volume, and $r - e_\alpha \delta t$ represents the position where the distribution function will stream to the interface after a time step δt .

To evaluate the flux \vec{F} by LBM, we can apply LBM to solve the local Riemann problem as shown in Fig. 1. At first, we calculate the conservative variables on both sides of interface by implementing an interpolation process. Then we further compute the corresponding equilibrium distribution function $g_L(r, t)$ and $g_R(r, t)$ by applying 1D compressible LB model. After that, we carry out a streaming step in the vicinity of interface. According to the streaming directions of lattice velocities, the equilibrium distribution function at the interface gives

$$g_{\alpha, \text{interface}}(r, t) = \begin{cases} \frac{1}{2}(g_{\alpha, L}(r - e_{\alpha} \delta t, t - \delta t) + g_{\alpha, R}(r - e_{\alpha} \delta t, t - \delta t)), & \text{if } e_{\alpha, \text{interface}} = 0, \\ g_{\alpha, L}(r - e_{\alpha} \delta t, t - \delta t), & \text{if } e_{\alpha, \text{interface}} > 0, \\ g_{\alpha, R}(r - e_{\alpha} \delta t, t - \delta t), & \text{if } e_{\alpha, \text{interface}} < 0, \end{cases} \quad (2.7)$$

where, $g_{\alpha, \text{interface}}$ and $e_{\alpha, \text{interface}}$ are the equilibrium distribution function and the lattice velocity at the interface, respectively. When the streaming time step δt indefinitely approaches zero, Eq. (2.7) becomes

$$g_{\alpha, \text{interface}}(r, t) = \begin{cases} \frac{1}{2}(g_{\alpha, L}(r, t) + g_{\alpha, R}(r, t)), & \text{if } e_{\alpha, \text{interface}} = 0, \\ g_{\alpha, L}(r, t), & \text{if } e_{\alpha, \text{interface}} > 0, \\ g_{\alpha, R}(r, t), & \text{if } e_{\alpha, \text{interface}} < 0. \end{cases} \quad (2.8)$$

Hereto, the equilibrium distribution function at the interface only relates to $g_L(r, t)$ and $g_R(r, t)$. For a certain stencil of LB model, Eq. (2.8) can be further simplified since the directions of lattice velocities are always perpendicular to the interface. As far as D1Q4 model (shown in Fig. 3) is concerned, Eq. (2.8) can be rewritten as

$$g_{\alpha, \text{interface}}(t) = \begin{cases} g_{\alpha, L}(t), & \text{if } \alpha = 1, 3, \\ g_{\alpha, R}(t), & \text{if } \alpha = 2, 4. \end{cases} \quad (2.9)$$

Eq. (2.9) is the 1D equilibrium distribution function model used in FV-LBM. However, it can also be employed for multi-dimensional problems. The technique is to apply the 1D model (Eq. (2.9)) along the normal direction of interface. Firstly, we calculate the flux vectors attributed to the normal velocity vector \vec{U}_n . By using the conservation forms of moments, the mass flux, normal component of the momentum flux and energy flux result from

$$F^n = \begin{cases} \rho U_n = \sum_{i=1}^N g_i e_i, \\ (\rho U_n U_n + p)[n_x, n_y, n_z]^T = [n_x, n_y, n_z]^T \sum_{i=1}^N g_i e_i e_i, \\ \left[\rho \left(\frac{p}{(\gamma - 1)\rho} + \frac{1}{2} U_n^2 \right) + p \right] U_n = \sum_{i=1}^N e_i g_i \left(\frac{1}{2} e_i e_i + \lambda \right), \end{cases} \quad (2.10)$$

where, λ is the potential energy of particles. Now, we consider the contribution of the remaining tangential velocity vector \vec{U}_τ to the flux vectors. Since \vec{U}_τ (here

$\vec{U}_\tau = (U_{\tau x}, U_{\tau y}, U_{\tau z})$ is parallel to the interface, it only produces momentum flux and energy flux, i.e.,

$$F^\tau = \begin{cases} 0, \\ \rho U_n [U_{\tau x}, U_{\tau y}, U_{\tau z}]^T, \\ \frac{1}{2} \rho U_n U_\tau^2. \end{cases} \tag{2.11}$$

By adding F^n and F^τ , we can get the total convective flux vectors at the interface as follows

$$F = \begin{bmatrix} \sum_{i=1}^N g_i e_i \\ \sum_{i=1}^N g_i e_i e_i \cdot n_x + F_1 \cdot U_{\tau x} \\ \sum_{i=1}^N g_i e_i e_i \cdot n_y + F_1 \cdot U_{\tau y} \\ \sum_{i=1}^N g_i e_i e_i \cdot n_z + F_1 \cdot U_{\tau z} \\ \sum_{i=1}^N e_i g_i \left(\frac{1}{2} e_i e_i + \lambda \right) + \frac{1}{2} F_1 \cdot |\vec{U}_\tau|^2 \end{bmatrix}, \tag{2.12}$$

where, F_1 is the first component of the flux vector F , that is, $\sum_{i=1}^N g_i e_i$.

From Eq. (2.12), it is clear that the component of equilibrium distribution function associated with the rest particle does not contribute to the flux vectors because of its zero lattice velocity. As a result, the case of $e_{\alpha, \text{interface}} = 0$ in Eq. (2.8) can be ignored for any configuration of lattice Boltzmann models. After flux vectors are evaluated by Eq. (2.12), Eq. (2.1) can be solved by conventional methods such as Runge-Kutta scheme.

2.2 The platform for constructing non-free parameter compressible LB model

The DVBE with BGK collision model [23] is given by

$$\frac{\partial f_\alpha}{\partial t} + \zeta_\alpha \cdot \nabla f_\alpha = \frac{(g_\alpha - f_\alpha)}{\tau_0}, \tag{2.13}$$

where, τ_0 is the single relaxation time. ζ_α is the lattice velocity, which corresponds to e_α in Eq. (2.5).

Usually, the equilibrium distribution function g is chosen as Maxwellian function. To recover compressible Euler equations from Eq. (2.13), g needs to satisfy the follow-

ing conservation forms of moments [14]

$$\int g d\zeta = \rho, \quad \int g \zeta_\alpha d\zeta = \rho u_\alpha, \quad \int g \zeta_\alpha \zeta_\beta d\zeta = \rho u_\alpha u_\beta + p \delta_{\alpha\beta}, \quad (2.14a)$$

$$\int g (\zeta_\alpha \zeta_\alpha + 2\lambda) d\zeta = \rho (u_\alpha u_\alpha + bRT), \quad (2.14b)$$

$$\int g (\zeta_\alpha \zeta_\alpha + 2\lambda) \zeta_\beta d\zeta = \rho [u_\alpha u_\alpha + (b + 2)RT] u_\beta, \quad (2.14c)$$

where, u_α and T are velocity in the α th direction and temperature of the mean flow, respectively. R is the specific gas constant. b is a given constant expressed as $b = 2/(\gamma - 1)$. Here, the specific heat ratio γ is tunable as a result of b chosen freely.

In the framework of lattice Boltzmann method, the integrals in Eq. (2.14) can be replaced by summations. As a result, for the one-dimensional case, Eq. (2.14) can be simplified to

$$\rho = \sum_\alpha g_\alpha, \quad \rho u = \sum_\alpha g_\alpha \zeta_\alpha, \quad \rho u^2 + p = \sum_\alpha g_\alpha \zeta_\alpha \zeta_\alpha, \quad (2.15a)$$

$$\rho (u^2 + bRT) = \sum_\alpha g_\alpha \zeta_\alpha \zeta_\alpha + 2\lambda \sum_\alpha g_\alpha, \quad (2.15b)$$

$$\rho [u^2 + (b + 2)RT] u = \sum_\alpha g_\alpha \zeta_\alpha \zeta_\alpha \zeta_\alpha + 2\lambda \sum_\alpha g_\alpha \zeta_\alpha. \quad (2.15c)$$

By substituting the first and the third relations into the fourth relation of Eq. (2.15), the potential energy of particles λ is obtained as

$$\lambda = \frac{(b - 1)}{2} RT = \left[1 - \frac{D}{2} (\gamma - 1) \right] e, \quad (2.16)$$

where, D denotes the space dimension, $D = 1$ means one-dimensional. e represents the potential energy of the mean flow, i.e., $e = p/(\gamma - 1)\rho$. By substituting expression (2.16) into Eq. (2.15), we can get the zeroth to third order of the conservation forms of moments as follows

$$\rho = \sum_\alpha g_\alpha, \quad \rho u = \sum_\alpha g_\alpha \zeta_\alpha, \quad (2.17a)$$

$$\rho u^2 + \rho c^2 = \sum_\alpha g_\alpha \zeta_\alpha \zeta_\alpha, \quad \rho u^3 + 3\rho u c^2 = \sum_\alpha g_\alpha \zeta_\alpha \zeta_\alpha \zeta_\alpha, \quad (2.17b)$$

where, c is the peculiar velocity of particles defined as

$$c = \sqrt{D(\gamma - 1)e}.$$

In current method, the equilibrium distribution functions associated with lattice velocities are considered as unknowns, and they are directly solved from Eq. (2.17).

This is an inverse problem. In fact, equation system (2.17) forms a basic platform to derive 1D compressible LB model, in which both the equilibrium distribution functions and lattice velocities are determined from conservation forms of moments.

2.3 Three non-free parameter one-dimensional compressible LB models

2.3.1 Non-free parameter D1Q3 model

If we set the distribution of the discrete lattice velocities as shown in Fig. 2, the resultant form of Eq. (2.17) gives

$$\rho = g_1 + g_2 + g_3, \quad \rho u = g_2 \cdot d - g_3 \cdot d, \quad (2.18a)$$

$$\rho u^2 + \rho c^2 = g_2 \cdot d^2 + g_3 \cdot d^2, \quad \rho u^3 + 3\rho uc^2 = g_2 \cdot d^3 - g_3 \cdot d^3. \quad (2.18b)$$

Note that, Eq. (2.18) provides four independent relations, which can be used to determine four unknowns g_1, g_2, g_3 and d . The result of system (2.18) is the non-free parameter D1Q3 model, i.e.,

$$g_1 = \frac{2\rho c^2}{d^2}, \quad g_2 = \frac{\rho(c^2 + u^2 + ud)}{2d^2}, \quad g_3 = \frac{\rho(c^2 + u^2 - ud)}{2d^2}, \quad (2.19a)$$

$$d = \sqrt{u^2 + 3c^2}. \quad (2.19b)$$

2.4 Non-free parameter D1Q4 model

The non-free parameter D1Q4 model is shown in Fig. 3. If the equilibrium density distribution functions and lattice velocities are considered as unknowns, we have six unknowns for this case (4 equilibrium distribution functions g_1, g_2, g_3, g_4 and 2 lattice velocities d_1, d_2). However, as indicated in the above section, equation system (2.17) only provides 4 independent relations for 1D case. Thus, we need two additional relations to close the system. This can be made by using the following two higher order conservation forms of moments [24,25], i.e.,

$$\rho u^4 + 6\rho u^2 c^2 + 3\rho c^4 = \sum_{\alpha} g_{\alpha} \tilde{\zeta}_{\alpha} \tilde{\zeta}_{\alpha} \tilde{\zeta}_{\alpha} \tilde{\zeta}_{\alpha}, \quad (2.20a)$$

$$\rho u^5 + 10\rho u^3 c^2 + 15\rho u c^4 = \sum_{\alpha} g_{\alpha} \tilde{\zeta}_{\alpha} \tilde{\zeta}_{\alpha} \tilde{\zeta}_{\alpha} \tilde{\zeta}_{\alpha} \tilde{\zeta}_{\alpha}. \quad (2.20b)$$

The first expression of Eq. (2.20) is actually the constraint needed to recover N-S equations from LBE and the second relation is associated with Burnett correction to heat flux. Since the additional equations can mimic the real physics, it is easy for the D1Q4

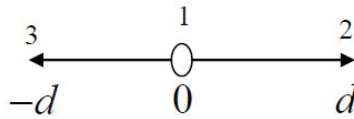


Figure 2: Distribution of discrete lattice velocities for D1Q3 model.

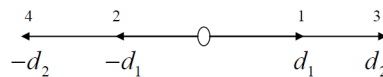


Figure 3: Distribution of discrete lattice velocities for D1Q4 model.

model to ensure positive density and pressure in the case of strong shocks and discontinuities. By combining Eq. (2.17) with Eq. (2.20), we can obtain the close-form equation system for D1Q4 model as follows

$$\rho = g_1 + g_2 + g_3 + g_4, \tag{2.21a}$$

$$\rho u = g_1 \cdot d_1 - g_2 \cdot d_1 + g_3 \cdot d_2 - g_4 \cdot d_2, \tag{2.21b}$$

$$\rho u^2 + \rho c^2 = g_1 \cdot d_1^2 + g_2 \cdot d_1^2 + g_3 \cdot d_2^2 + g_4 \cdot d_2^2, \tag{2.21c}$$

$$\rho u^3 + 3\rho u c^2 = g_1 \cdot d_1^3 - g_2 \cdot d_1^3 + g_3 \cdot d_2^3 - g_4 \cdot d_2^3, \tag{2.21d}$$

$$\rho u^4 + 6\rho u^2 c^2 + 3\rho c^4 = g_1 \cdot d_1^4 + g_2 \cdot d_1^4 + g_3 \cdot d_2^4 + g_4 \cdot d_2^4, \tag{2.21e}$$

$$\rho u^5 + 10\rho u^3 c^2 + 15\rho u c^4 = g_1 \cdot d_1^5 - g_2 \cdot d_1^5 + g_3 \cdot d_2^5 - g_4 \cdot d_2^5. \tag{2.21f}$$

By using the well-known software Matlab or Maple, the equilibrium distribution functions and lattice velocities of this model can be easily derived as

$$g_1 = \frac{\rho(-d_1 d_2^2 - d_2^2 u + d_1 u^2 + d_1 c^2 + u^3 + 3uc^2)}{2d_1(d_1^2 - d_2^2)}, \tag{2.22a}$$

$$g_2 = \frac{\rho(-d_1 d_2^2 + d_2^2 u + d_1 u^2 + d_1 c^2 - u^3 - 3uc^2)}{2d_1(d_1^2 - d_2^2)}, \tag{2.22b}$$

$$g_3 = \frac{\rho(d_1^2 d_2 + d_1^2 u - d_2 u^2 - d_2 c^2 - u^3 - 3uc^2)}{2d_2(d_1^2 - d_2^2)}, \tag{2.22c}$$

$$g_4 = \frac{\rho(d_1^2 d_2 - d_1^2 u - d_2 u^2 - d_2 c^2 + u^3 + 3uc^2)}{2d_2(d_1^2 - d_2^2)}, \tag{2.22d}$$

$$d_1 = \sqrt{u^2 + 3c^2 - \sqrt{4u^2 c^2 + 6c^4}}, \tag{2.22e}$$

$$d_2 = \sqrt{u^2 + 3c^2 + \sqrt{4u^2 c^2 + 6c^4}}. \tag{2.22f}$$

2.4.1 Non-free parameter D1Q5 model

The configuration of D1Q5 model is shown in Fig. 4. For this case, we have 7 unknowns (5 equilibrium distribution functions g_1, g_2, g_3, g_4, g_5 and 2 lattice velocities d_1, d_2). Thus, apart from 6 relations used in the derivation of D1Q4 model, we need 1 more relation. This can be given by the sixth order conservation form of moments [24, 25]. Thus, the corresponding well-posed equation system of D1Q5 model can be written as

$$\rho = g_1 + g_2 + g_3 + g_4 + g_5, \tag{2.23a}$$

$$\rho u = g_2 \cdot d_1 - g_3 \cdot d_1 + g_4 \cdot d_2 - g_5 \cdot d_2, \tag{2.23b}$$

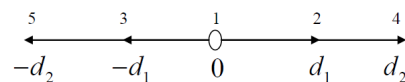


Figure 4: Distribution of discrete lattice velocities for D1Q5 model.

$$\rho u^2 + \rho c^2 = g_2 \cdot d_1^2 + g_3 \cdot d_1^2 + g_4 \cdot d_2^2 + g_5 \cdot d_2^2, \quad (2.23c)$$

$$\rho u^3 + 3\rho u c^2 = g_2 \cdot d_1^3 - g_3 \cdot d_1^3 + g_4 \cdot d_2^3 - g_5 \cdot d_2^3, \quad (2.23d)$$

$$\rho u^4 + 6\rho u^2 c^2 + 3\rho c^4 = g_2 \cdot d_1^4 + g_3 \cdot d_1^4 + g_4 \cdot d_2^4 + g_5 \cdot d_2^4, \quad (2.23e)$$

$$\rho u^5 + 10\rho u^3 c^2 + 15\rho u c^4 = g_2 \cdot d_1^5 - g_3 \cdot d_1^5 + g_4 \cdot d_2^5 - g_5 \cdot d_2^5, \quad (2.23f)$$

$$\rho u^6 + 15\rho u^4 c^2 + 45\rho u c^4 + 15\rho c^6 = g_2 \cdot d_1^6 + g_3 \cdot d_1^6 + g_4 \cdot d_2^6 + g_5 \cdot d_2^6. \quad (2.23g)$$

Then a non-free parameter D1Q5 model can be given as

$$g_1 = \frac{\rho(d_1^2 d_2^2 - d_1^2 u^2 - d_1^2 c^2 - d_2^2 u^2 - d_2^2 c^2 + u^4 + 6u^2 c^2 + 3c^4)}{d_1^2 d_2^2}, \quad (2.24a)$$

$$g_2 = \frac{\rho(-d_1 d_2^2 u - d_2^2 u^2 - d_2^2 c^2 + d_1 u^3 + 3d_1 u c^2 + u^4 + 6u^2 c^2 + 3c^4)}{2d_1^2(d_1^2 - d_2^2)}, \quad (2.24b)$$

$$g_3 = \frac{\rho(d_1 d_2^2 u - d_2^2 u^2 - d_2^2 c^2 - d_1 u^3 - 3d_1 u c^2 + u^4 + 6u^2 c^2 + 3c^4)}{2d_1^2(d_1^2 - d_2^2)}, \quad (2.24c)$$

$$g_4 = \frac{\rho(d_2 d_1^2 u + d_1^2 u^2 + d_1^2 c^2 - d_2 u^3 - 3d_2 u c^2 - u^4 - 6u^2 c^2 - 3c^4)}{2d_2^2(d_1^2 - d_2^2)}, \quad (2.24d)$$

$$g_5 = \frac{\rho(-d_2 d_1^2 u + d_1^2 u^2 + d_1^2 c^2 + d_2 u^3 + 3d_2 u c^2 - u^4 - 6u^2 c^2 - 3c^4)}{2d_2^2(d_1^2 - d_2^2)}, \quad (2.24e)$$

$$d_1 = \sqrt{u^2 + 5c^2 - \sqrt{4u^2 c^2 + 10c^4}}, \quad (2.24f)$$

$$d_2 = \sqrt{u^2 + 5c^2 + \sqrt{4u^2 c^2 + 10c^4}}. \quad (2.24g)$$

2.5 Positivity property of three models

From the physical point of view, the equilibrium density distribution function g_α represents the mass of particles with the lattice velocity e_α . Naturally, it should be a positive quantity. In D1Q3 model, it is easy to prove that g_1, g_2 and g_3 are always positive if the local Mach number is less than $\sqrt{1/\gamma}$. Similarly, the condition of D1Q4 and D1Q5 models for keeping positive g_α can be derived as the local Mach number being less than $\sqrt{0.75/\gamma}$ and $\sqrt{2.137/\gamma}$, respectively. Note that, a negative component of the equilibrium distribution functions does not definitely produce unstable resolution. The reason is that the calculated density is the summation of all equilibrium density distribution functions, which could still positive even when a negative equilibrium distribution function appears.

From the above expressions, it can be easily revealed that only g_3 in D1Q3 model, g_4 in D1Q4 model and g_3 in D1Q5 model will become negative with the gradually increasing Mach number from zero to infinity. Fig. 5 shows the variation tendency of the values of these three equilibrium distribution functions with Mach number. Here, the density and specific heat ratio are set as 1 and 1.4, respectively. As shown in Fig. 5, although the critical value of Mach number of g_4 in D1Q4 model (decreasing to zero)

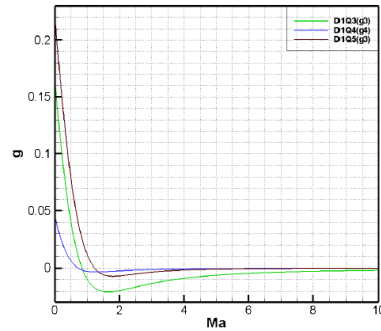


Figure 5: Values of equilibrium distribution functions vary with Mach number.

is less than those of g_3 in D1Q3 and D1Q5 models, the minimum value of g_4 is more close to positive. This property will help D1Q4 model to enhance the computational stability, especially for simulation of hypersonic flows with strong shocks and discontinuities. Besides, we can conclude that these three equilibrium distribution functions would finally tend to zero when the flow velocity is infinity.

3 Numerical examples

To validate the capability of the FV-LBM and investigate the performance of the three non-free parameter models (D1Q3, D1Q4 and D1Q5), some 1D and 2D compressible inviscid flows are simulated. All the computations were done on PC-Core II 2.0GHz.

3.1 Sod shock tube

The first test case is the Sod shock tube. When the diaphragm is broken ($t = 0$), a shock wave propagates to the right part and an expansion wave propagates to the left part. The initial value of this problem is set as

$$\begin{cases} (\rho_L, u_L, p_L) = (1, 0, 1), & -0.5 < x < 0, \\ (\rho_R, u_R, p_R) = (0.125, 0, 0.1), & 0 < x < 0.5. \end{cases} \quad (3.1)$$

In this case, reference density and reference length are set as $\rho_0 = 1$ and $L_0 = 1$, respectively. The mesh size is chosen as $\Delta x = 1/250$ and the time step size is taken as $\Delta t = 0.001$. Fig. 6 shows the computed density, velocity, pressure, and internal energy profiles by D1Q3 model (green dashed lines with delta symbols), D1Q4 model (blue dash dot lines with gradient symbols) and D1Q5 model (purple dash double dots lines with diamond symbols). Meanwhile, the exact solutions are also presented as red solid lines for comparison. Clearly, results of the three non-free parameter models agree fairly well with each other and can essentially match with the exact solution. However, D1Q3 model is more efficient as it requires less computational time with 0.12500s as compared to 0.15625s by D1Q4 model and 0.17188s by D1Q5 model.

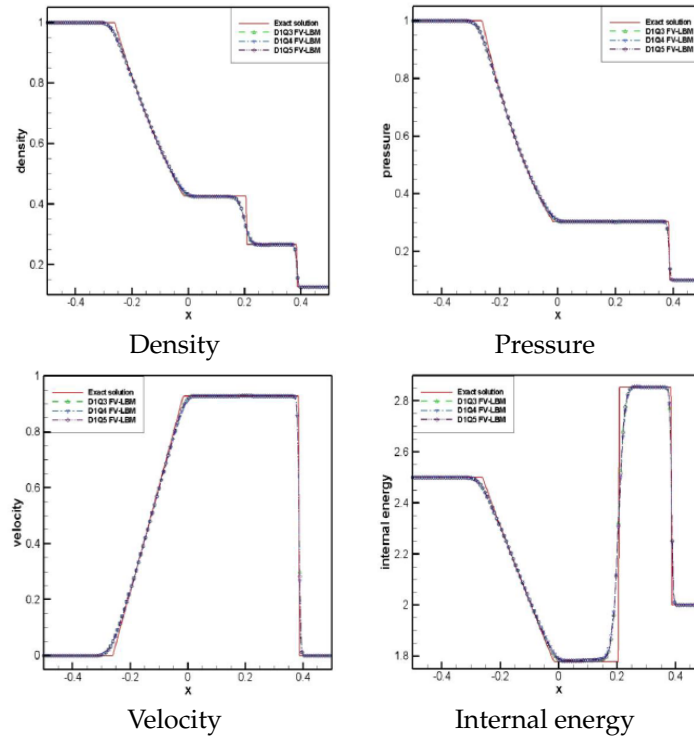


Figure 6: Comparison of density, pressure, velocity, and internal energy profiles for the Sod shock tube problem at time $t = 0.22$.

3.2 Lax shock tube

The second test case is also a shock tube problem, in which the initial condition is given as

$$\begin{cases} (\rho_L, u_L, p_L) = (0.445, 0.698, 3.528), & -0.5 < x < 0, \\ (\rho_R, u_R, p_R) = (0.5, 0, 0.571), & 0 < x < 0.5. \end{cases} \quad (3.2)$$

In this case, the reference variables, mesh size, time step size and graphic instructions are taken to be the same as those of the Sod shock tube problem. The computed results are shown in Fig. 7. Once again, the present results of the three models are in good agreement with the exact solution. Similarly, D1Q3 model is more efficient which only consumes 0.26562s as compared to 0.31250s by D1Q4 model and 0.34375s by D1Q5 model.

3.3 Implosion problem

To illustrate the ability of the FV-LBM for multi-dimensional problems, the implosion problem is studied. It is an unsteady flow in a two-dimensional container. Inside the container, the gases at rest are separated into two regions with a central square

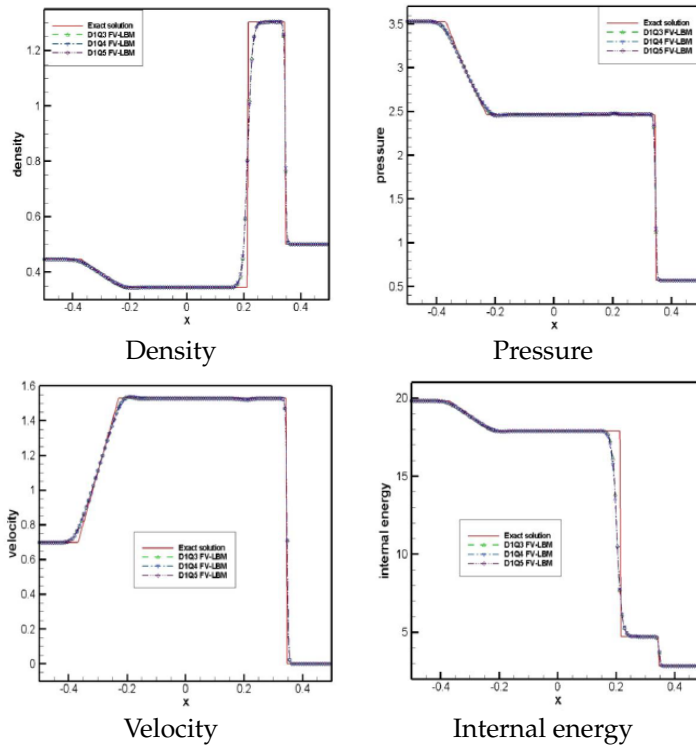


Figure 7: Comparison of density, pressure, velocity, and internal energy profiles for the Lax shock tube problem at time $t = 0.14$.

diaphragm. The initial values in the two domains are shown in Fig. 8. At time $t = 0$, the diaphragm is ruptured, and the inner and outer gases begin to interact with each other. Since the flow is confined by solid walls, it will be reflected from the walls continuously and become more and more complex. In our test, uniform mesh size of 200×200 is used. The computed pressure and Mach number contours at $t = 0.8$ are shown in Fig. 9. To make comparison, the results obtained by Roe scheme [18] are also presented in the figure. Obviously, the results of the FV-LBM are basically the same as those of Roe scheme. Also noteworthy, D1Q3 model requires less computational time with 747.20s as compared to 813.33s by D1Q4 model and 836.25s by D1Q5 model.

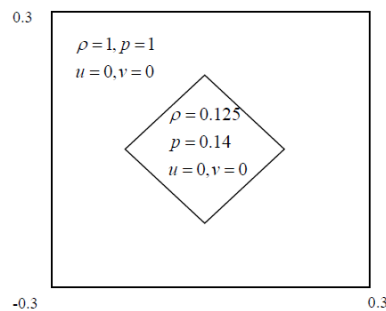
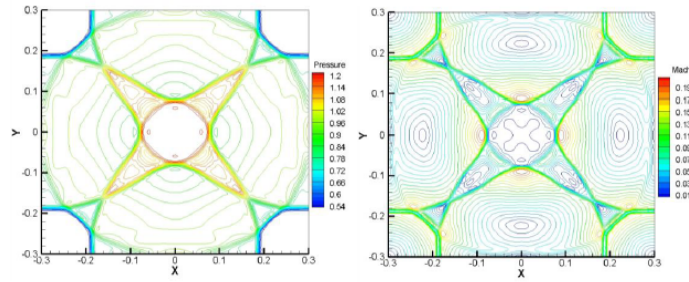
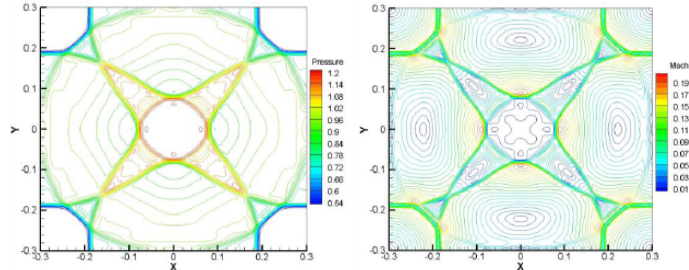


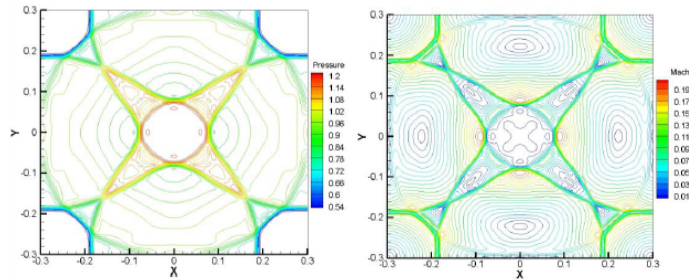
Figure 8: The initial condition and geometry of the implosion problem.



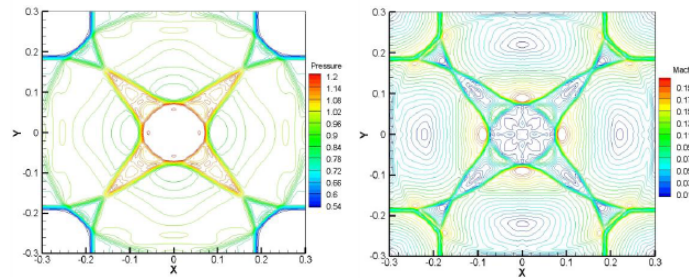
(a) The results of D1Q3 model



(b) The results of D1Q4 model



(c) The results of D1Q5 model

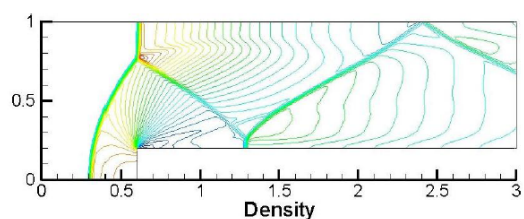


(d) The results of Roe scheme

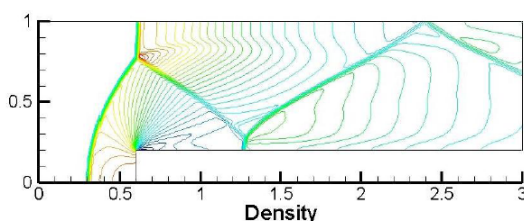
Figure 9: Comparison of pressure (left) and Mach number (right) contours for the implosion problem.

3.4 Forward facing step problem

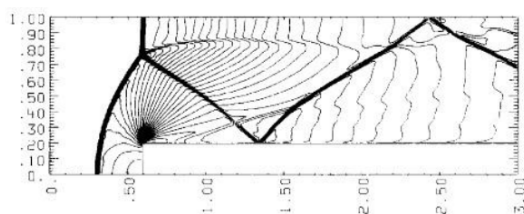
In this test, we consider a stationary Mach 3 flow hitting a rectangular step. The formulation of this problem, computational setup and detailed discussion of the flow physics can be found in reference [26]. In the computation, the uniform mesh size



(a) The results of D1Q4 model



(b) The results of D1Q5 model



(c) The results of literature [26]

Figure 10: Comparison of density contours for the forward facing step problem.

of 300×100 is used. It must be pointed out that D1Q3 model can not work for this test case due to the fact that the density and pressure at cells near the corner become negative after a few iterations. The reason may be that it is more difficult for D1Q3 model to guarantee the positivity property of the density and pressure in this region since the minimum value of equilibrium distribution function of D1Q3 model is less than those of D1Q4 and D1Q5 models. Fig. 10 shows the density contour computed by D1Q4 model and D1Q5 model. Also presented in the figure is the result of Woodward and Colella [26]. Clearly, both the results of D1Q4 model and D1Q5 model are in good agreement with the results in [26]. However, D1Q4 model is more efficient as it requires less computational time with 1094.84s as compared to 1117.44s by D1Q5 model.

3.5 Supersonic flows around a diamond airfoil

The last test case is the compressible inviscid flow around a diamond airfoil with different free-stream Mach number. It is a self-design test problem, which is applied to assess the accuracy, convergence rate and application range of Mach number of the three non-free parameter models. In current simulation, only the top half of the airfoil is considered in view of symmetrical characteristics of the airfoil. The angle of attack is

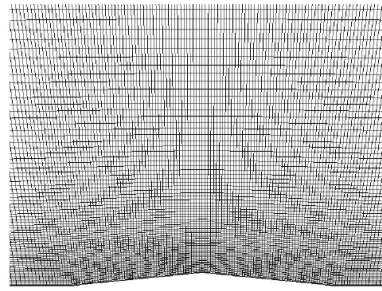


Figure 11: Partial view of the grid around a diamond airfoil.

set as 0 degree. The thickness ratio of the diamond airfoil is 0.1. The non-uniform grid with cell number of 20000 is used, and its partial view is shown in Fig. 11. Figs. 12-14 show the pressure contours, pressure coefficient distribution on the airfoil surface and convergence history computed by the three models, respectively. As can be seen from Figs. 12 and 13, the results computed by D1Q3 model show some oscillation as compared with those of D1Q4 and D1Q5 models. The reason may be due to the fact that the auxiliary constraints of D1Q4 and D1Q5 models give more physical results than D1Q3 model. Additionally, from the convergence history (Fig. 14) of the three models, we can see that D1Q4 and D1Q5 models have a faster convergence rate than D1Q3 model for a given convergence threshold.

The application range of free-stream Mach number of the three models is relevant to the interpolation scheme used to evaluate the macroscopic variables at cell interface. When the second-order interpolation scheme is applied, and Venkatakrishnan’s limiter [27, 28] is used, the permitted free-stream Mach number of the three models are basically the same and all can reach about 6. However, if only the first-order interpolation scheme is used, the feasible free-stream Mach number of D1Q4 and D1Q5 models is unlimited. On the other hand, D1Q3 model only reaches about 8. The results indicate that the permitted free-stream Mach number is mainly determined by the minimum value of equilibrium distribution function. For the computational cost of the three models, it was found that D1Q3 model requires 1180.9s, and D1Q4

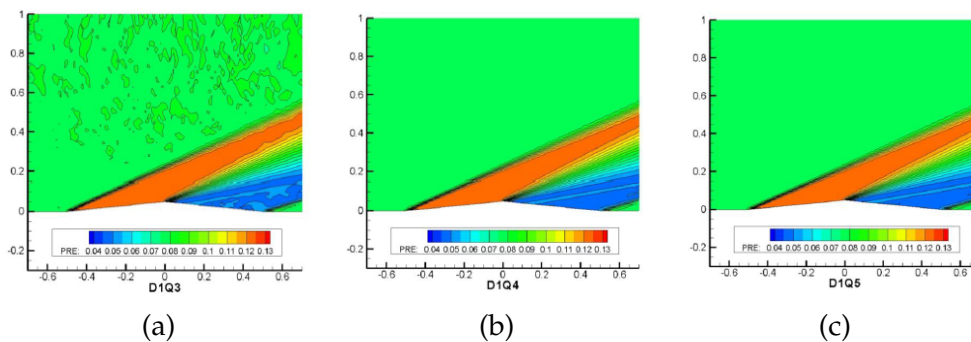


Figure 12: Comparison pressure contours of D1Q3 model (a), D1Q4 model (b) and D1Q5 model (c) for flows around a diamond airfoil.

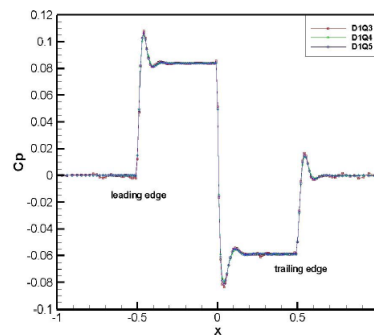


Figure 13: Pressure coefficient distribution on the diamond airfoil surface.

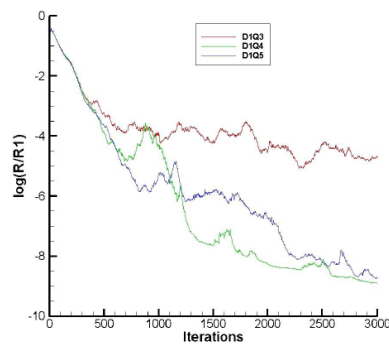


Figure 14: Convergence history of D1Q3 model, D1Q4 model and D1Q5 model for flows around a diamond airfoil.

and D1Q5 models need 1290.9s and 1321.8s respectively for 3000 iterations. From the above results, it is clear that both D1Q4 and D1Q5 models are suitable for simulating hypersonic flows. However, when the computational effort is taken into account, D1Q4 model is superior to D1Q5 model.

4 Conclusions

In this paper, the details of finite volume-based lattice Boltzmann method (FV-LBM) are presented. FV-LBM basically solves the macroscopic Euler equations, but the convective fluxes at the cell interface are evaluated by applying the one-dimensional compressible lattice Boltzmann model along the normal direction. The approach combines the advantages of both FVM and LBM.

To develop one-dimensional compressible lattice Boltzmann models used in FV-LBM, the paper presents a platform, which is formed from the conservation forms of various order moments. In the platform, both the equilibrium distribution functions and the lattice velocities are considered as unknowns and solved from the platform. Furthermore, the paper presents three typical non-free parameter models, D1Q3, D1Q4 and D1Q5, under the platform. At the same time, the positivity property of the three models is analyzed briefly.

By applying FV-LBM together with three proposed models, several numerical examples including 1D and 2D problems have been well simulated. The obtained results indicated that all models can work well for compressible inviscid flows. From the comparison, it was exhibited that the D1Q3 model has the highest computational efficiency and the D1Q4 and D1Q5 models give the wider application range of Mach number. Specifically, we found that the D1Q4 model is the optimal choice for the FV-LBM simulation of hypersonic flows as compared with D1Q3 and D1Q5 models.

References

- [1] A. NABOVATI, D. P. SELLAN AND C. H. AMON, *On the lattice Boltzmann method for phonon transport*, J. Comput. Phys., 230 (2011), pp. 5864–5876.
- [2] O. MALASPINAS, N. FIETIER AND DEVILLE, *Lattice Boltzmann method for the simulation of viscoelastic fluid flows*, J. Non-Newtonian. Fluid. Mech., 165 (2010), pp. 1637–1653.
- [3] J. WU AND C. SHU, *A solution-adaptive lattice Boltzmann method for two-dimensional incompressible viscous flows*, J. Comput. Phys., 230 (2011), pp. 2246–2269.
- [4] D. RICOT, S. MARIE, P. SAGAUT AND C. BAILLY, *Lattice Boltzmann method with selective viscosity filter*, J. Comput. Phys., 228 (2009), pp. 4478–4490.
- [5] X. HE AND L. S. LUO, *Lattice Boltzmann model for the incompressible Navier-Stokes equation*, J. Stat. Phys., 88 (1997), pp. 927–944.
- [6] Z. L. GUO, B. C. SHI AND N. C. WANG, *Lattice BGK model for the incompressible Navier-Stokes equation*, J. Comput. Phys., 165 (2000), pp. 288–306.
- [7] H. XU, W. Q. TAO AND Y. ZHANG, *Lattice Boltzmann model for three-dimensional decaying homogeneous isotropic turbulence*, Phys. Lett. A., 373 (2009), pp. 1368–1373.
- [8] S. CHEN, *A large-eddy-based lattice Boltzmann model for turbulent flow simulation*, Appl. Math. Comput., 215 (2009), pp. 591–598.
- [9] T. INAMURO, T. OGATA, S. TAJIMA AND N. KONISHI, *A lattice Boltzmann method for incompressible two-phase with large density differences*, J. Comput. Phys., 198 (2004), pp. 628–644.
- [10] K. N. PREMNATH AND J. ABRAHAM, *Three-dimensional multi-relaxation time (MRT) lattice Boltzmann models for multiphase flow*, J. Comput. Phys., 224 (2007), pp. 539–559.
- [11] M. MEHRAVARAN AND S. K. HANNANI, *Simulation of incompressible two-phase flows with large density differences employing lattice Boltzmann and level set methods*, Comput. Methods. Appl. Mech. Eng., 198 (2008), pp. 223–233.
- [12] T. KATAOKA AND M. TSUTAHARA, *Lattice Boltzmann method for the compressible Euler equations*, Phys. Rev. E., 69 (2004), 056702.
- [13] T. KATAOKA AND M. TSUTAHARA, *Lattice Boltzmann method for the compressible Navier-Stokes equations with flexible specific-heat ratio*, Phys. Rev. E., 69 (2004), R035701.
- [14] K. QU, C. SHU AND Y. T. CHEW, *Alternative method to construct equilibrium distribution functions in lattice-Boltzmann method simulation of inviscid compressible flows at high Mach number*, Phys. Rev. E., 75 (2007), 036706.
- [15] K. QU, C. SHU AND Y. T. CHEW, *Simulation of shock-wave propagation with finite volume lattice Boltzmann method*, Int. J. Mod. Phys. C., 18 (2007), pp. 447–454.
- [16] Q. LI, Y. L. HE, Y. WANG AND W. Q. TAO, *Coupled double-distribution-function lattice Boltzmann method for the compressible Navier-Stokes equations*, Phys. Rev. E., 76 (2007), 056705.

- [17] C. Z. JI, C. SHU AND N. ZHAO, *A lattice Boltzmann method-based flux solver and its application to solve shock tube problem*, Mod. Phys. Lett. B., 23 (2009), pp. 313–316.
- [18] P. L. ROE, *Approximate Riemann solvers, parameter vectors and difference schemes*, J. Comput. Phys., 43 (1981), pp. 357–372.
- [19] B. VAN LEER, *Flux vector splitting for the Euler equations*, Lect. Notes. Phys., 170 (1982), pp. 507–512.
- [20] M. S. LIOU AND C. J. STEFFEN, *A new flux vector splitting scheme*, J. Comput. Phys., 107 (1993), pp. 23–39.
- [21] M. S. LIOU, *A sequel to AUSM: AUSM+*, J. Comput. Phys., 129 (1996), pp. 364–382.
- [22] M. S. LIOU, *A sequel to AUSM, part II: AUSM+-up for all speeds*, J. Comput. Phys., 214 (2006), pp. 137–170.
- [23] P. L. BHATNAGAR, E. P. GROSS AND M. KROOK, *A model for collision processes in gases. I: small amplitude processes in charged and neutral one-component systems*, Phys. Rev., 94 (1954), pp. 511–525.
- [24] K. XU, *A gas-kinetic BGK scheme for the compressible Navier-Stokes equations*, NASA/CR, 38 (2000), 210544.
- [25] K. XU, *A gas-kinetic BGK scheme for the Navier-Stokes equations and its connection with artificial dissipation and Godunov method*, J. Comput. Phys., 171 (2001), pp. 289–335.
- [26] P. WOODWARD AND P. COLELLA, *The numerical simulation of two-dimensional fluid flow with strong shocks*, J. Comput. Phys., 54 (1984), pp. 115–173.
- [27] V. VENKATAKRISHNAN, *On the accuracy of limiters and convergence to steady state solutions*, AIAA Paper, (1993), 93-0880.
- [28] V. VENKATAKRISHNAN, *Convergence to steady-State solutions of the Euler equations on unstructured grids with limiters*, J. Comput. Phys., 118 (1995), pp. 120–130.